Available online at www.sciencedirect.com
ScienceDirect
Trans. Nonferrous Met. Soc. China 20(2010) 1829−1834
Transactions of Nonferrous Metals Society of China
www.tnmsc.cn

Electron beam welding of Ti-15-3 titanium alloy to 304 stainless steel with copper interlayer sheet

WANG Ting(王 廷), ZHANG Bing-gang(张秉刚), CHEN Guo-qing(陈国庆),
FENG Ji-cai(冯吉才), TANG Qi(唐 奇)

State Key Laboratory of Advanced Welding Production Technology, Harbin Institute of Technology, Harbin 150001, China

Received 27 November 2009; accepted 22 March 2010

Abstract: Electron beam welding of Ti-15-3 titanium alloy to 304 stainless steel with a copper sheet as interlayer was carried out. Microstructures of the joint were studied by optical microscopy (OM), scanning electron microscopy (SEM) and X-ray diffractometry (XRD). In addition, the mechanical properties of the joint were evaluated by tensile test and the microhardness was measured. These two alloys were successfully welded by adding copper transition layer into the weld. Solid solution with a certain thickness was located at the interfaces between weld and base metal in both sides. Regions inside the weld and near the stainless steel were characterized by solid solution of copper with $TiFe_2$ intermetallics dispersedly distributed in it. While weld near titanium alloy contained Ti-Cu and Ti-Fe-Cu intermetallics layer, in which the hardness of weld came to the highest value. Brittle fracture occurred in the intermetallics layer when the joint was stretched.
Key words: Ti-15-3 titanium alloy; 304 stainless steel; electron beam welding; intermetallics layer; mechanical properties

1 Introduction

Recently, composite structures of dissimilar metals were gradually appreciated in national defense and civil industrial fields, such as aeronautics and astronautics, energy and electric power industry. Composite components of titanium alloy and steel can fully exert the advantages of these two materials simultaneously. Partial replacement of steel components by titanium alloy will become an important approach to reduce mass of spacecrafts[1−2].

Fusion welding of titanium alloy and steel was difficult to implement for the production of brittle phases in weld[3−4]. Research work of TIG welding of pure titanium and pure iron showed that the basic reason for the embrittlement of the joint was the emergence of continuously distributed TiFe, $TiFe_2$ and eutectic structure. Hardness of weld metal was in the range of HV 740−1324[5]. So far, less literature about successful fusion welding of these two alloys has been reported. Inversely, pressure welding and brazing can eliminate the problems in fusion welding because the base metals remain in the solid state during joining. Furthermore, many successful examples were reported[6−8]. However, the service conditions may make particular processes unsuitable. For high temperature applications, brazing cannot be candidate. Furthermore, the required joint geometry can make friction welding and explosive welding difficult to apply[9−10].

Owing to the advantages of high energy density, precisely controllable heating position and radius, electron beam welding was the most frequently utilized fusion welding method in the field of joining of dissimilar metals[11]. Based on the successful research results of the electron beam welding of copper alloy to stainless steel and titanium alloy[12−13], a copper interlayer sheet was adopted in the present work to join Ti-15-3 titanium alloy and 304 stainless steel by electron beam welding. Meanwhile, the microstructure, phase constitution and mechanical properties of the joint were analyzed.

2 Experimental

Materials applied in this experiment was β type titanium alloy Ti-15-3 and 304 austenitic stainless steel. Their chemical composition, physical and mechanical

Corresponding author: WANG Ting; Tel: +86-13059015199; E-mail: fgwangting@163.com
DOI: 10.1016/S1003-6326(09)60381-2

properties are given in Tables 1−3. From Table 3 we could see that there were great differences in thermal conductivity and linear expansion coefficient between two base metals, which would lead to large temperature gradient and thermal stress in joint during the welding process. The metals were machined into 50 mm × 25 mm × 2.5 mm plates, then mechanically and chemically cleaned before welding. 1 mm-thick copper sheet was adopted as transition layer and placed at the contact face, then fixed by spot welding using TIG method.

Table 1 Chemical composition of Ti-15-3 titanium alloy (mass fraction, %)

Al	Cr	Sn	V	Ti
2.8−3.6	2.5−3.5	2.5−3.5	14.0−16.0	Bal.

Table 2 Chemical composition of 304 stainless steel (mass fraction, %)

C	Ni	Cr	Mn	Si	Fe
≤0.07	8−11	17−19	≤2.0	≤1.0	Bal.

Table 3 Physical properties and tensile strength of Ti-15-3 titanium alloy and 304 stainless steel

Material	Melting point/°C	Tensile strength/MPa	Specific heat capacity/ ($J\cdot kg^{-1}\cdot K^{-1}$)
Ti-15-3	1700	975	536
304	1450	550	502

Material	Thermal conductivity/ ($W\cdot m^{-1}\cdot K^{-1}$)	Linear expansion coefficient/($10^{-6}K^{-1}$)
Ti-15-3	6.1	8.9
304	14.6	16.0

Because the thickness of the copper layer is much larger than the heating radius of electron beam, dual-pass welding was conducted in order to make the transition materials melt sufficiently and mix with the melted base metal homogeneously. The first pass acted on the copper layer 0.3 mm away from the interface between titanium alloy and copper with welding parameters of accelerating voltage 55 kV, focus current 2 450 mA, welding speed 300 mm/min and beam current 9 mA. Then, the second pass acted on the interface between copper and stainless steel with beam current of 8 mA and the other parameters same as the first pass.

Samples for analyses were wire cut perpendicularly to welding direction from the welded joint, then ground and polished. Microstructure observation and composition measurement were implemented on a S4700 type scanning electron microscope made in Hitachi Company. Mechanical property of the joint was evaluated according to micro-hardness distribution along horizontal direction on the cross section and tensile test.

3 Results and discussion

3.1 Microstructure and composition

3.1.1 Formation of weld and macrostructure of cross section

Surface features of Ti-15-3/304 joints electron beam welded with and without inserting a copper transition sheet into contact face are shown in Fig.1. It is found that Ti-15-3 and 304 stainless steel plates could not be joined by electron beam welding method without the assistance of copper interlayer. In fact, as discussed above, Ti-Fe intermetallics continuously distributed in direct fusion weld, resulting in great brittleness, so that the joint cracked under a relative low stress. But, when a copper interlayer was utilized, a crack-free joint was obtained by electron beam welding. It is easy to draw a conclusion that the addition of copper element into weld could improve the metallurgy condition which could optimize the plasticity and toughness of the joint.

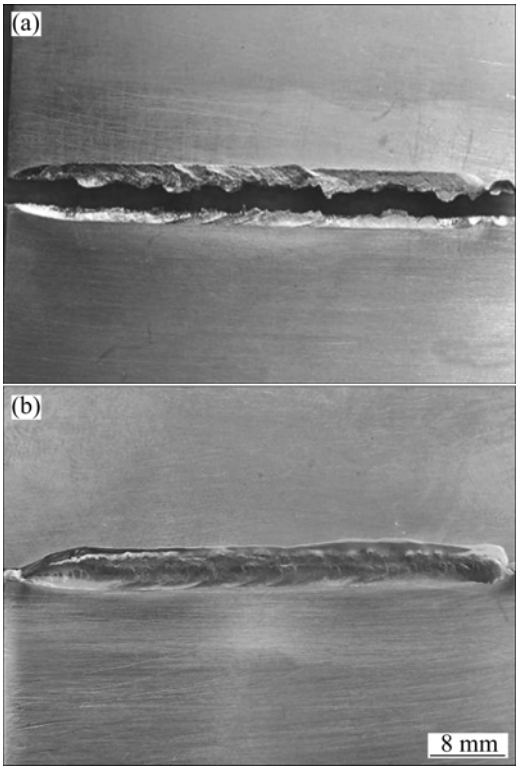

Fig.1 Surface features of Ti-15-3/304 joints electron beam welded without (a) and with (b) inserting copper transition sheet

Macrostructure of cross section of embedded copper interlayer in Ti-15-3/304 joint is shown in Fig.2. It is clear that the weld was characterized by full penetration and the joint was achieved by typical fusion welding

process. In other words, dissimilar joint of titanium alloy and stainless steel could be successfully welded by fusion welding owing to the addition of copper transition layer. Furthermore, it could also be seen that there was solid solution of copper uniformly distributed in weld, which helps to improve the plasticity of the joint. A bright reactive layer emerged in the vicinity of titanium alloy. It might consist of Ti-Cu intermetallics of lower brittleness than Ti-Fe intermetallics.

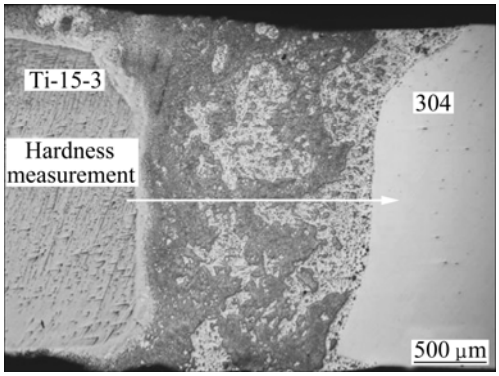

Fig.2 Macrostructure of cross section of weld

3.1.2 Microstructure and phase constitution

Research emphases in the present work were laid on the metallurgical reaction products and their distribution in weld, as well as their influence on the mechanical properties of the joint when copper was added. Therefore, the microstructure and phase constitution in various regions of weld as shown in Fig.3 were analyzed.

In the weld region near titanium alloy with greater chemical activity (Fig.3(a)), metallurgical reaction was complex, confirmed by large numbers of reaction products with a variety of morphology. This region could be divided into three reaction zones respectively marked as zone I, II and III according to their different morphological characteristics of the included reactive phases. Zone I consisted of white phase A, light gray phase B, dark gray phase C and gray black phase D. Among them A was located among B blocks, a bit of C lay inside B blocks, and D was dispersively distributed in each phase. Zone II contained three types of phases, i.e. big blocky dark gray phase E, light gray phase F which was distributed around E. Very little white phase G laid between E and F. There were two kinds of phases in zone III. One was dark gray phase H contacting with titanium alloy and the other was light gray phase I surrounded by H.

Microstructure in the weld center is shown in Fig.3(b). This region was located in the center of weld pool during welding process and liquid materials mixed uniformly there. Hence, metallurgical reaction was relatively simple. The white phase M was located among dark gray blocks marked by K, exhibiting a kind of net structure.

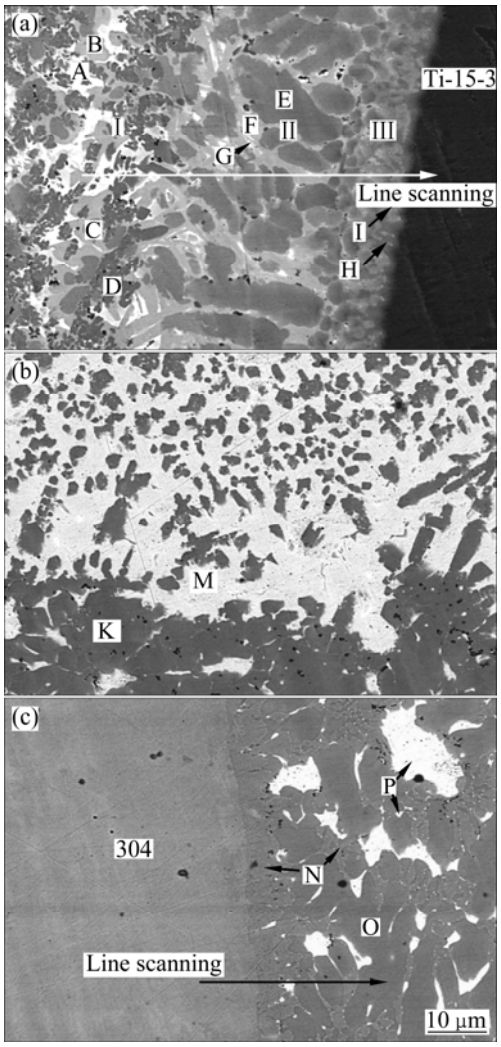

Fig.3 Microstructures of various regions in weld: (a) Beside titanium alloy; (b) Center; (c) Beside 304

Region beside 304 stainless steel consisted of three reaction products of different morphologies, i.e. fine gray phase N contacting with base metal, big blocky phase O of gray color and white phase P (Fig.3(c)). Moreover, phase P with great inhomogeneity of size was situated between phase N and O.

SEM-EDX analysis was applied to phases A−P to analyze the kinds of the reactive products in various weld regions. The compositions of main elements in each phase are listed in Table 4. Combined with Ti-Fe and Ti-Cu binary phase diagrams (Fig.4)[14−15], the kind of each phase could be deduced and the results are listed in Table 5. XRD analysis also confirmed the existence of them (Fig.5). In weld regions near titanium alloy, the reaction of Cu and Ti elements was the primary controlling metallurgical process with Ti-Cu intermetallics as reactive products. Zone I was a mixture of Ti-Cu compounds and solid solution of copper. While zones II and III only consisted of intermetallics layer, which would bring great brittleness to these two zones.

Table 4 Chemical compositions of phases (molar fraction, %)

Phase	Ti	Fe	Ni	Cu	Cr	V
A	10	5	3	72	5	5
B	38	7	2	45	5	3
C	44	20	1	22	4	9
D	34	29	1	6	15	15
E	41	20	2	21	6	10
F	36	6	2	46	6	4
G	28	7	1	56	4	5
H	66	5	1	14	2	12
I	44	4	1	45	2	4
K	28	49	3	4	11	5
M	15	3	7	74	1	0
N	6	57	5	5	20	7
O	30	50	3	3	11	3
P	10	8	6	72	4	0

Fortunately, weld center contained solid solution of copper with dispersed $TiFe_2$ compound interiorly. This distribution pattern of $TiFe_2$ could not only improve the plasticity of joint but also strengthen the relatively soft solid solution of copper. Likewise, there were solid solution of copper and iron with $TiFe_2$ dispersedly distributed interiorly in weld near stainless steel.

Comprehensive analysis could be performed now from above results. $TiFe_2$ blocks with large brittleness were dispersedly distributed in solid solution in the weld center and the vicinity of stainless steel. As a result, the plasticity of the electron beam welding joint between titanium alloy and stainless steel was improved significantly. For the interfaces between the weld and base metal in both sides, there was solid solution of a certain thickness. Although there were intermetallics in the weld near titanium alloy, they were composed of Ti-Cu and Ti-Fe-Cu compounds of lower brittleness than Ti-Fe compounds with a relatively small width. Dispersed distribution in solid solution of brittle $TiFe_2$ compound and the narrowing of intermetallics layer were the key reasons for the achievement of the crack-free Ti-15-3/304 fusion welding joint.

3.1.3 Linear distribution of main elements

In order to analyze the horizontal distribution of alloying elements on the two sides of fusion line during

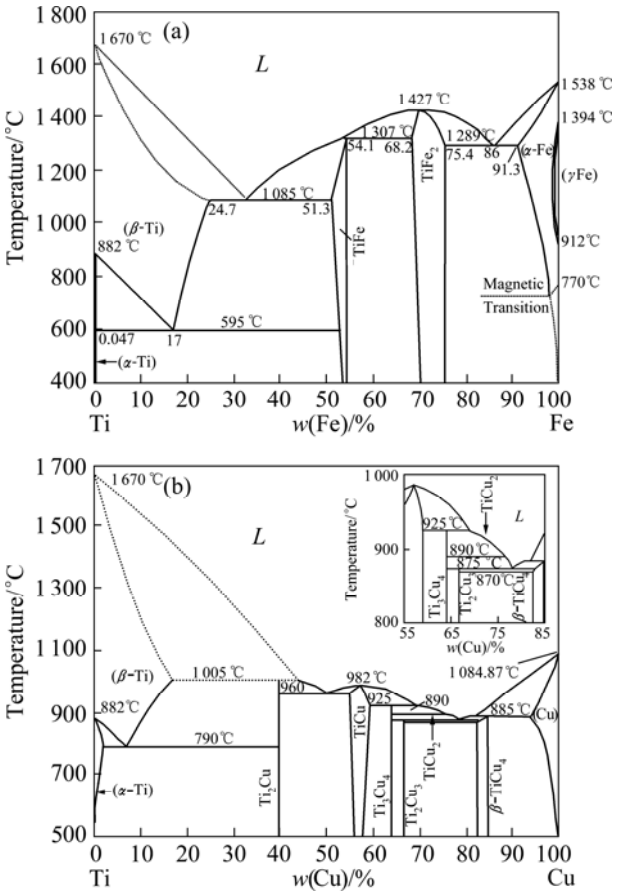

Fig.4 Ti-Fe (a) and Ti-Cu (b) binary phase diagrams

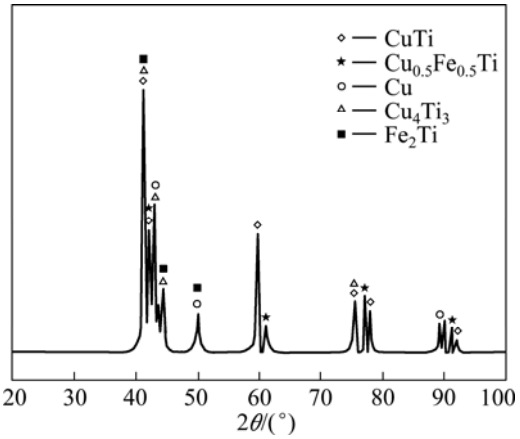

Fig.5 XRD pattern of intermetallics in joint

Table 5 Potential reacting phases in various regions

Weld near titanium alloy									Weld center		Weld near steel		
I				II			III						
A	B	C	D	E	F	G	H	I	K	M	N	O	P
Cu(ss)	Cu_4Ti_3 or CuTi	$Fe_{0.5}Cu_{0.5}Ti$	TiFe	$Fe_{0.5}Cu_{0.5}Ti$	Cu_4Ti_3 or CuTi	Cu_2Ti	Ti(ss)+ Ti_2Cu	Cu_4Ti_3 or CuTi	$TiFe_2$	Cu(ss)	Fe(ss)	$TiFe_2$	Cu(ss)

ss—Solid solution.

welding process, linear scanning analysis of the main elements was carried out on SEM. Scanning lines were marked in Figs.3(a) and 3(c). The distribution curve on the side of stainless steel is shown in Fig.6(a). There was a segment rich in Fe and Cr but poor in Ti. It was considered as solid solution of iron, which proved that there was no interfacial compound layer. The segment with high content of copper element corresponded to solid solution of copper. While segments with content ratio of Fe to Ti remaining approximately 2:1 corresponded to $TiFe_2$ blocks. This curve profile also confirmed the alternate distribution of $TiFe_2$ and solid solution. On the other side (Fig.6(b)), the content of Ti element rose quickly form one side to the other side of fusion line with a small slope, which demonstrated the emergence of a thin solid solution layer of titanium. Cu content fluctuating greatly in zone I showed that compounds were isolated by solid solution of copper. $Fe_{0.5}Cu_{0.5}Ti$ and Cu_4Ti_3 (or CuTi) were alternately distributed in zone II. Zone III consisted of Cu_4Ti_3 (or CuTi) and Ti_2Cu.

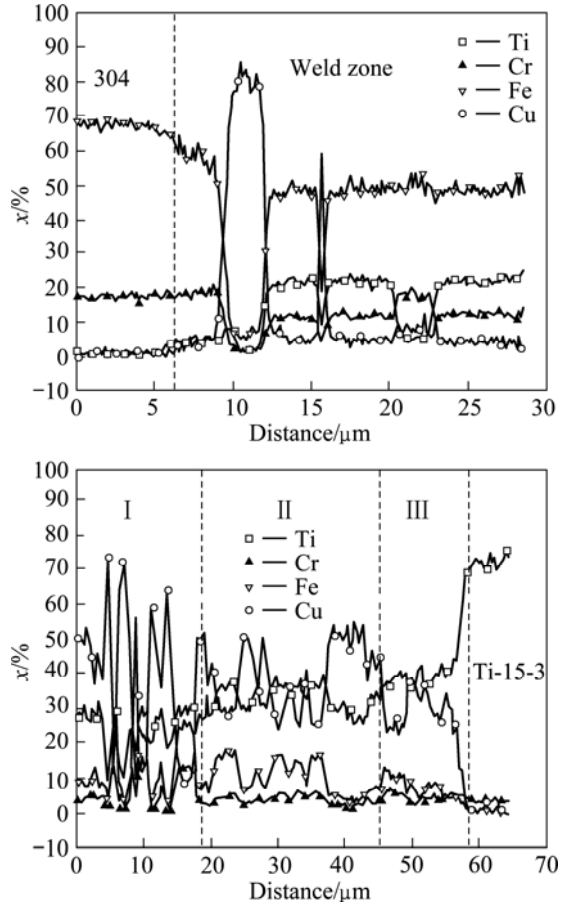

Fig.6 Horizontal distribution of main elements on two sides of fusion line: (a) Stainless steel side; (b) Titanium alloy side

3.2 Mechanical properties

3.2.1 Tensile strength and fracture surface

Tensile strength at room temperature was up to 224 MPa with a whole elongation of 3.6% of the joint under strain rate of 0.2 mm/min. It was shown that electron beam welded Ti-15-3/304 joint with a copper interlayer could obtain a certain strength, which could supply guidance to the fusion welding of titanium alloy and steel.

Fracture location of the joint is given in Fig.7. It could be seen that fracture occurred in the intermetallics layer near titanium alloy. Hence, the intermetallics layer was the weakest part of the joint and it should be paid more attention to improve the kinds and distribution of the included compounds in the subsequent research work. Fracture surface of the joint with sector pattern revealed brittle cleavage fracture mode (Fig.8).

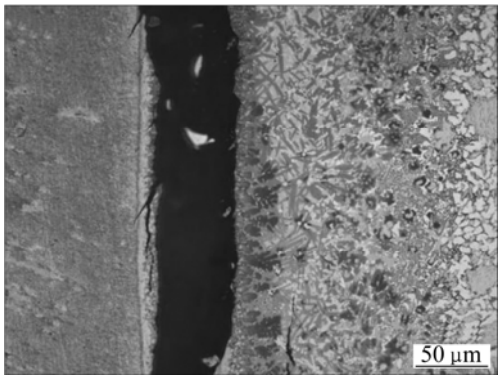

Fig.7 Fracture location of joint after stretching

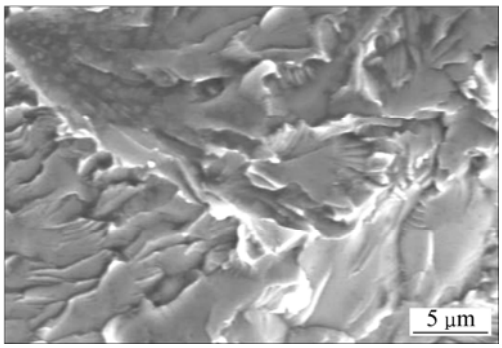

Fig.8 Micro-morphology of fracture surface

3.2.2 Microhardness

Microhardness distribution on cross section of the weld was measured along the path marked in Fig.2. The result is shown in Fig.9. Microhardness in the weld near stainless steel consisting of $TiFe_2$ and solid solution was higher than that of base metal. While it decreased slightly in the weld center because of the content increase of solid solution of copper. Microhardness came to the highest value in the intermetallics layer near titanium alloy, up to HV 700. Thus, the plasticity of this zone was the poorest. This result was corresponding to the tensile strength test.

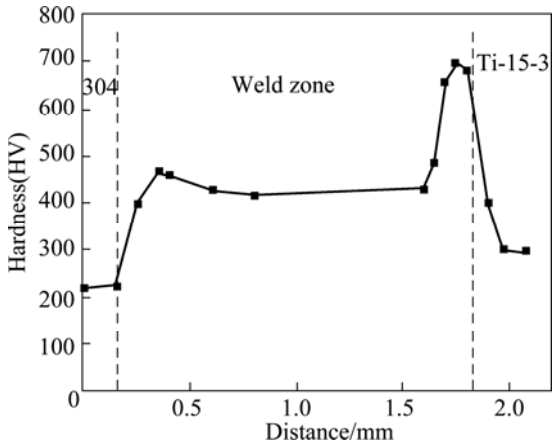

Fig.9 Microhardness distribution on cross section of weld

4 Conclusions

1) Crack free electron beam welding joint of Ti-15-3 and 304 titanium alloy could be successfully obtained by adding copper transition layer into the weld. The tensile strength could be up to 234 MPa with good surface configuration.

2) Dispersed distribution of brittle $TiFe_2$ compound in solid solution and the narrowing of intermetallics layer were the key reasons for success. The highest value of microhardness emerged in Ti-Cu and Ti-Cu-Fe compounds layer, where the welding joint ruptured complying brittle cleavage fracture mode when being stretched.

3) The intermetallics layer embrittled the joint seriously and more attention should be paid to improve the plasticity of welding joint in the subsequent research work.

References

[1] BOYER R R. An overview on the use of titanium in the aerospace industry [J]. Materials Science and Engineering A, 1996, 213(1/2): 103−114.

[2] YUAN X J, SHENG G M, QIN B. Impulse pressuring diffusion bonding of titanium alloy to stainless steel [J]. Materials Characterization, 2008, 59(7): 930−936.

[3] WANG Ting, ZHANG Bing-gang, CHEN Guo-qing, FENG Ji-cai. Problems and research status of welding between dissimilar titanium alloy and steel [J]. Welding and Joining, 2009(9): 29−33. (in Chinese)

[4] ELREFAEY A, TILLMANN W. Solid state diffusion bonding of titanium to steel using a copper base alloy as interlayer [J]. Journal of materials processing technology, 2008, 209(5): 2746−2752.

[5] LI Biao-feng. Study on the weldability of titanium and steel and titanium clad steel plate(I) [J]. Development and Application of Materials, 2004, 19(1): 41−44. (in Chinese)

[6] YUE X, HE P, FENG J C. Microstructure and interfacial reactions of vacuum brazing titanium alloy to stainless steel using an AgCuTi filler metal [J]. Materials Characterization, 2008, 59(12): 1721−1727.

[7] QIN B, SHENG G M, HUANG J W, ZHOU B. Phase transformation diffusion bonding of titanium alloy with stainless steel[J]. Materials Characterization, 2006, 56(1): 32−38.

[8] GHOSH M, CHATTERJEE S. Characterization of transition joints of commercially pure titanium to 304 stainless steel [J]. Materials Science and Technology, 2002, 48(5): 393−399.

[9] HE P, YUE X, ZHANG J H. Hot pressing diffusion bonding of a titanium alloy to a stainless steel with an aluminum alloy interlayer[J]. Materials Science and Engineering A, 2008, 486(1/2): 171−176.

[10] AKBARI MOUSAVI S A A, FARHADI SARTANGI P. Experimental investigation of explosive welding of cp-titanium/AISI 304 stainless steel [J]. Materials and Design, 2009, 30(3): 459−468.

[11] SUN Z, KARPPI R. The application of electron beam welding for the joining of dissimilar metals: An overview [J]. Journal of Materials Processing Technology, 1996, 59(3): 257−267.

[12] ZHANG Bing-gang, HE Jin-shan, FENG Ji-cai. Microstructures and formation of electron beam welding joint of QCr0.8 and 1Cr21Ni5Ti [J]. The Chinese Journal of Nonferrous Metals, 2004, 14(9): 1569−1574. (in Chinese)

[13] MAGNABOSCO I, FERRO P, BONOLLO F. An investigation of fusion zone microstructure in electron beam welding of copper-stainless steel [J]. Materials Science and Engineering A, 2006, 224(1/2): 163−173.

[14] OKAMOTO H. Fe-Ti(iron-titanium)[J]. Journal of Phase Equilibria, 1996, 17(4): 369.

[15] MURRAY J L. The Cu-Ti(copper-titanium) system[J]. Journal of Phase Equilibria, 1983, 4(1): 81−95.

(Edited by YANG Bing)